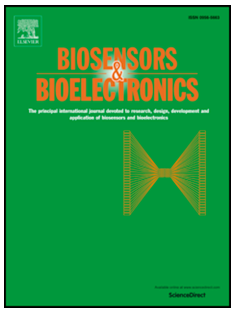

Coenzyme A-aptamer-facilitated label-free electrochemical stripping strategy for sensitive detection of histone acetyltransferase activity

Dandan Hu, Yufang Hu, Tianyu Zhan, Yudi Zheng, Pingjian Ran, Xinda Liu, Zhiyong Guo, Wenting Wei, Sui Wang

PII: S0956-5663(19)31012-7

DOI: https://doi.org/10.1016/j.bios.2019.111934

Reference: BIOS 111934

To appear in: *Biosensors and Bioelectronics*

Received Date: 27 September 2019

Revised Date: 11 November 2019

Accepted Date: 26 November 2019

Please cite this article as: Hu, D., Hu, Y., Zhan, T., Zheng, Y., Ran, P., Liu, X., Guo, Z., Wei, W., Wang, S., Coenzyme A-aptamer-facilitated label-free electrochemical stripping strategy for sensitive detection of histone acetyltransferase activity, *Biosensors and Bioelectronics* (2020), doi: https://doi.org/10.1016/j.bios.2019.111934.

Coenzyme A-aptamer-facilitated label-free electrochemical stripping strategy for sensitive detection of histone acetyltransferase activity

Dandan Hu[a], Yufang Hu[a, b, *], Tianyu Zhan[a], Yudi Zheng[a], Pingjian Ran[a], Xinda Liu[a], Zhiyong Guo[a], Wenting Wei[a], Sui Wang[a, *]

[a] State Key Laboratory for Managing Biotic and Chemical Threats to the Quality and Safety of Agro-products, State Key Laboratory Base of Novel Functional Materials and Preparation Science, School of Materials Science & Chemical Engineering, Ningbo University, Ningbo, Zhejiang 315211, PR China

[b] State Key Laboratory of Chemo/Biosensing and Chemometrics, College of Chemistry and Chemical Engineering, Hunan University, Changsha, Hunan 410082, PR China

*Corresponding author. Phone: +86-574-87600798. Fax: +86-574-87600798. E-mail: huyufang@nbu.edu.cn, wangsui@nbu.edu.cn.

Abstract

Abnormal histone acetyltransferases (HAT) activity gives rise to all kinds of cellular diseases. Herein, we first report a coenzyme A (CoA)-aptamer-facilitated label-free electrochemical stripping biosensor for sensitive detection of HAT activity via square wave voltammetry (SWV) technique. The presence of HAT can lead to the transfer of the acetyl group from acetyl coenzyme A (Ac-CoA) to lysine residues of substrate peptide, thus generating CoA molecule. Later, CoA, which acts as an initiator, can embrace its aptamer via the typical target-aptamer interaction, then arousing deoxynucleotide terminal transferase (TdT)-induced silver nanoclusters (AgNCs) as signal output. Under optimized conditions, the resultant aptasensor shows obvious electrochemical stripping signal and is employed for HAT p300 analysis in a wide concentration range from 0.01 to 100 nM with a very low detection limit of 0.0028 nM (3δ/slope). The good analytical performances of the biosensor depend on the strong interaction of CoA and its aptamer and abundant stripping resource rooted from AgNCs. Next, the proposed biosensor is used for screening HAT's inhibitors and the practical HAT detection with satisfactory results. Therefore, the new, simple and sensitive HAT biosensor presents a promising direction for HAT-targeted drug discovery and epigenetic research.

Keywords: Histone acetyltransferase; Coenzyme A-aptamer; Electrochemical stripping detection; Screening of inhibitors

1. Introduction

Plenty of posttranslational modifications play key roles in eukaryotic transcription and regulating chromatin dynamics, in where is located in the histone proteins with flexible and highly conserved N-terminus (Magiera et al., 2018; Langelier et al., 2018; Compton et al., 2018). Generally, acetylation, methylation, ubiquitination, phosphorylation, sumoylation and ADP-ribosylation are some common posttranslational modifications (Chuh, 2016; Qi et al., 2019). Thereinto, histone acetylation is an important modification in gene transcription, which is regulated by histone acetyltransferase (HAT) (Luan et al., 2019; Bennett et al., 2019). HAT is a class of enzyme, which can catalyze the occurrence of acetylation reaction within the core histone proteins (a transfer of an acetyl group from acetyl-CoA (Ac-CoA) to the specific lysine residues) (Michaelides et al., 2018; Lee et al., 2019). Moreover, in 1994, it was first cloned to identify a protein, which can bind E1A and is also an adenoviral oncogenic transcription factor (Zucconi et al., 2019; Michaelides et al., 2018). Majority of HATs involves in many cellular processes, such as gene silencing, chromosome assembly, DNA replication/repair, cell cycle regulation, and transcriptional activation (McCullough et al., 2016; Sen et al., 2019). In this regard, the sensitive analysis of HAT may be a promising way for clinical serious diseases diagnoses, and the detection method still require further improvement.

As far, all kinds of techniques have been developed to probe HAT activity. Traditional detection methods for HAT activity depend on the autoradiography and radio isotopes (Ait-Si-Ali et al., 1998), which suffer from hazards of radioactive

materials. Later, fluorescent (Ghadiali et al., 2011; Chen et al., 2015; Wang et al., 2017; Han et al., 2015), electrochemiluminescence (Zou et al., 2018; Zou et al., 2019; Miao et al., 2019; Chen et al., 2019; Hu et al., 2019) and electrochemical (Xu et al., 2019; Hu et al., 2015) methods for HAT activity come along successively. It is worth mentioning that the recent interest has been moved to the use of miniaturized devices from a sophisticated laboratory diagnosis, presenting the potentiality of point-of-care. Based on it, electrochemical method stands out from other methods due to its own unique benefits involving high sensitivity, low-cost, ease of use and possibility of miniaturization (Zhang et al., 2018; Goda et al., 2019; Asadian et al., 2019). Different electrochemical technologies for HAT have been reported except square wave voltammetry (SWV), which originally developed by Kalousek and Barker (Barker et al., 1992; Yin, et al., 2019), and the detection of HAT by SWV method has been rarely reported. Therefore, it is desired to propose a SWV biosensor for HAT detection with high sensitivity in the development process of a point-of-care platform.

Aptamer, which is a kind of short single-stranded DNA or RNA, is normally identified from a random library comprised of approximately 10^{12}-10^{14} unique oligonucleotides of 20-80 bases by a procedure known as Systematic Evolution of Ligands by Exponential Enrichment (SELEX) *in vitro* process (Akki et al., 2018; Vázquez-González et al., 2018). Meanwhile, it is well-known bio-receptor that can have high affinity and specificity with target molecule (Yan et al., Xiong et al., 2019; Nie et al., 2019). Actually, compared with antibody, aptamer has plenty of advantages, including low cost, ease of synthesis and modification, excellent thermal stability and

short of immunogenicity and toxicity, and it is more suitable to be used as molecular probes for a biosensor (Zhu et al., 2018; Yaghoub et al., 2019; Ahmadyousefi et al., 2019). Because of these advantages, aptamer even wins potential application in the fabrication of various biosensors (Espiritu et al., 2018; Weerathunge et al., 2019; Ma et al., 2019; Naveen Kumar et al., 2018; Singh et al., 2018). However, it has been few studies about aptamer-guided HAT-target biosensors.

On this basis, we propose a novel SWV aptasensor by utilizing the interaction between CoA molecule and its aptamer and deoxynucleotide terminal transferase (TdT)-induced silver nanoclusters (AgNCs) for sensitive detection of HAT activity (p300 as a model of HAT) for the first time. On the one hand, in this aptasensor, CoA molecules are released by HAT-based catalysis, in which the acetyl group was transferred from Ac-CoA to lysine residues on the substrate peptide. On the other hand, CoA molecules are captured by CoA-aptamer immobilized onto the Au electrode surface. After the treat of Exo I, CoA-aptamer can be still extended by TdT-based catalytic reaction, and the generated rich-C DNA could act as the template of AgNCs. As a result, the as-fabricated AgNCs are introduced as the electrochemical stripping signal to monitor CoA molecule. On the contrary, the absence of CoA leads to the Exo I-caused degradation of CoA-aptamer, and thus subsequent other processes are static. Based on the relationship between CoA molecule and HAT p300, HAT p300 and its inhibitors can be also quantified with high sensitivity by our SWV platform. The proposed strategy presents a novel method for HATs activity detection, which is helpful for further development of a miniaturized and low-cost electrochemical

sensing platform for clinic diagnosis and drug discovery.

2. Experimental

2.1. Materials and apparatus

Substrate peptide, CoA-aptamer and its control DNAs, whose sequences were displayed in Table S1, were prepared by Sangon Biotech. Co. Ltd. (Shanghai, China). Coenzyme A (CoA), acetyl coenzyme A (Ac-CoA), HAT (p300, >95%, SDS-PAGE, solution in 50 mM Tris-HCl, pH 7.5, containing 100 mM sodium chloride, 0.2% NP-40, 50 mM imidazole, and 10% glycerol), exonuclease I (Exo I), protein kinase A (PKA), cholesterol oxidase (ChOx), and anacardic acid were obtained from Sigma-Aldrich (Shanghai, China). Terminal deoxynucleotidyl transferase (TdT, carried reaction buffer: 1 M potassium cacodylate, 0.125 M Tris, 0.05% (v/v) Triton X-100, 5 mM $CoCl_2$ (pH 7.2)), diethyl pyrocarbonate (DEPC) water, horseradish peroxidase (HRP), deoxycytidine triphosphate (dCTP), adenosine triphosphate (ATP), adenine, and adenosine monophosphate (AMP) were obtained from Shanghai Sangon Biotechnology Co. Ltd. (Shanghai, China). Uracil-DNA glycocasylase (UDG), chymotrypsin (CHY) and acetyl cholinesterase (AChE) were purchased from Aladdin Industrial Corporation. C646 was purchased from Selleck in China (Shanghai, China). All other reagents were at analytical grade or better. CoA-aptamer-related solutions were prepared with DEPC water, but other ones were prepared with double-distilled water (18.25 MΩ cm) from the Millipore Milli-Q system. All buffers used in our work were given in the supporting information.

All electrochemical experiments including square wave voltammetry (SWV), cyclic voltammetry (CV) and electrochemical impedance spectroscopy (EIS) were performed on a CHI 760E electrochemical workstation (Chenhua Instrument Company of Shanghai, China) and a conventional three-electrode system. The gold electrode (2 mm in diameter) served as the working electrode. A platinum wire electrode and a saturated Ag/AgCl electrode were employed as the counter and reference electrode, respectively. Electrochemical detection was performed by SWV within the potential range from +0.06 to +0.24 V with the following parameters: amplitude, 0.025 V; frequency, 15 Hz. Electrochemical characterizations were carried out by cyclic voltammetry (CV) from -0.1 to +0.5 V with a scan rate of 50 mV/s and electrochemical impedance spectroscopy (EIS) with the frequency of 10^5 to 10^{-2} Hz at amplitude of 5 mV in 5 mM $[Fe(CN)_6]^{3-/4-}$ containing 0.1 M KCl. Fluorescence spectra were measured at room temperature in a 100 μL quartz cuvette on a Hitachi F-4600 spectrometer (Hitachi Co. Ltd., Japan). Polyacrylamide gel electrophoresis (PAGE) was scanned by a ChemiDoc™ MP System, Bio-Rad, USA. The morphology and chemical composition of the DNA-AgNCs were examined with a JEM-2100F high resolution transmission electron microscope (HR-TEM) and a Multimode 8 AFM (Bioscope system, Brucker).

2.2. Fabrication of CoA aptamer-facilitated HAT biosensor

Bare Au: Prior to modification, bare gold electrode (Au, 2 mm diameter) was carefully polished on a chammy with 0.3 and 0.05 μm alumina slurry, followed by sequentially sonication for 5 min each in water, ethanol, and double-distilled water.

After that, the polished gold electrode was treated with prepared piranha solution (H_2SO_4/H_2O_2, 3:7 by volume) for 10 min and rinsed with double-distilled water thoroughly.

Electrode 1: CoA-aptamer-2 was dissolved in DNA immobilization buffer, yielding a final concentration of 1 μM. Then, this solution was heated to 95 °C for 2 min, then cooled to 4 °C over 30 s, using a T100^{TM} thermal cycler (Bio-Rad, USA). Then, 3 μL of aptamer probe was added to the cleaned gold electrode and allowed to react overnight at room temperature. After being rinsed with double-distilled water, 2-mercaptoethanol (1 mM) was dropped onto the electrode surface for 30 min to remove nonspecific adsorption sites.

Electrode 2: 2.5 μL of CoA (100 μM) were incubated on the surface of Electrode 1 at 37 °C for 30 min, and then a 2.5 μL Exo I (0.5 U/mL) solution was pipetted at the above electrode surface at 37 °C for 30 min.

Electrode 3: After Exo I cleavage, TdT reaction solution including 0.5 μL dCTP (10 mM), 0.1 μL TdT (10 U/mL), 1 μL 5×TdT buffer, and double-distilled water (0.9 μL) was dropped and incubated at 37 °C for 60 min. Later, 2.5 μL $AgNO_3$ (0.1 mM) and 2.5 μL fresh $NaBH_4$ solution (0.1 mM) were added onto the electrode surface and put in dark for 30 min at room temperature. After washing with double-distilled water, the resulting electrode was subjected to the electrochemical measurements.

2.3. Probing HAT p300 activity

HAT p300 detection was carried out by the generation of CoA. For HAT activity analysis, p300 with different concentrations, 1 μL Ac-CoA (1 mM) and 0.4 μL peptide

(1 mM) were added into phosphate buffer (10 mM, pH 7.0) with a total volume of 2 μL at 30 °C for 80 min under stirring, diluting the resulting solution 10 times. After acetylation reaction, the mixture was added on the Electrode 1 surface, and other experimental procedures were as same as the ones of "Electrode 1-3".

For inhibitor screening experiments, a series of anacradic acid or C646 samples were extra added into the above acetylation reaction solution and other experimental procedures were as same as the ones of "HAT p300 detection" above.

3. Results and discussion

3.1. Design strategy

In this work, we take advantage of CoA as an initiator to develop a novel strategy for investigating HAT p300 activity and the entire principle is illustrated in Scheme 1. The detection mechanism is dependent of three fascinating discoveries: (1) It is well known, aptamer can optionally bind target molecule with high affinity and specifically. So, the appearance of CoA-aptamer provides great potential for CoA-related biosensing, however, biosensing strategy involving the interaction of CoA molecule and its aptamer has not yet been reported; (2) HAT p300 catalyzes the transfer of an acetyl group from Ac-CoA to lysine residue of substrate peptide, producing ε-N-acetyl lysine residue and CoA. In the presence of HAT p300, the produced CoA is expected to get in touch with CoA-aptamer to achieve HAT p300 activity detection indirectly; (3) Stripping voltammetry is one of the most useful electro-analytical

strategies for trace level determinations, and SWV is one of the most suitable techniques for electrochemical biosensor platform. At this point, TdT-derived DNA-AgNCs can provide a powerful stripping resource. For another, the combination by integrating stripping voltammetry with SWV for HAT p300 detection has not yet been found. Based on these recoveries, a novel, label-free and sensitive HAT p300 biosensor is investigated by employing TdT-derived AgNCs as stripping signal output. Moreover, some inhibitors could hinder the acetylation process, it is of significance on the development of HAT-related disease-relevant drug screening.

3.2. Feasibility study

To verify the affinity of CoA and its aptamer, four-relevant DNAs (their sequences are given in Table S1) are selected for specificity tests by fluorescent measurements. Based on the interaction of graphene (GO) with DNAs (Han et al., 2015), 5'-6-carboxyfluorescein (FAM)-labelled DNA adsorbed onto GO can trigger fluorescence resonance energy transfer (FRET) between FAM and GO, where FAM acts as an excited donor fluorophore and GO serves as an acceptor fluorophore through long-range dipole-dipole interactions for the detection of CoA. As shown in Figure 1A, a series of FAM-labeled DNAs with sequence specificity (DNA1, DNA2, DNA3 and CoA-aptamer-1) are mixed with CoA, respectively, and their fluorescence intensities change with the adsorption time, showing a gradual downward trend. Moreover, the fluorescence of DNA1, DNA2, and DNA3 shows the fastest fluorescence drop, while the one of CoA-aptamer-1 only decreases slightly. Those results indicate that the presence of CoA hinders the combination of DNAs and GO,

that is CoA-aptamer-1 has a high affinity for CoA. For another, some substances similar with CoA are also investigated for the special binding. As illustrated in Figure 1B, only is CoA present, the fluorescence signal is relatively obvious, and otherwise the change of the target gives rise to the quenching of the fluorescence signal due to the binding of the free DNA and GO. Later, we compare the signals again under CoA with different concentrations. As can be seen from Figure 1C, the amount of CoA has an effect on the fluorescence intensity measurements such that when the amount of CoA is less, the fluorescence of FAM is not enough determined. This result may be because less combination of CoA to CoA-aptamer-1 may lead to more adsorption of CoA-aptamer-1 and GO. To further explore the interaction, the same experiments are conducted under different concentrations of NaCl. As depicted in Figure 1D, fluorescence quenching decreases with increasing NaCl concentration, one likely reason is that there is a better combination of CoA and its aptamer at 100 mM NaCl. These results lay a solid foundation for the follow-up experiments in our work.

(Figure 1)

AgNCs serve as the signal putout, which have a pivotal position in our HAT biosensor. So, some characterization experiments, such as polyacrylamide gel electrophoresis (PAGE), atomic force microscopy (AFM), and transmission electron microscope (TEM), are employed for proving the formation of AgNCs. First, we use a non-denaturing gel electrophoresis to characterize the formation of TdT-based rich-C DNA, which is the template of AgNCs. As shown in Figure S1A, compared with sole CoA-aptamer-2 (lane 2, clear band), a long and trailing band is observed for

TdT-yielded DNA (lane 3), what's more, a bright smear band with quite large molecular weight appears at lane 4, revealing the formation of DNA-template AgNCs as designed. To further explore it, AFM is also employed to this formation and "cotton balls" arise on mica substrate (Figure S1B), actually, it is because DNA-template AgNCs occur conformational change from long linear chain to football-shaped bunches under water shortage. Later, it can be seen that pieces of tanglesome AgNCs are displayed in Figure S1C, but AgNCs with approximately 2 nm come forth clearly in its inset, indicating their high specific area. Finally, as shown in Figure S1D, TdT-grown AgNCs display an excitation peak centered at 497 nm and an emission peak centered at 562 nm. These results suggest a well-formed DNA-template AgNCs.

In view of the interaction between CoA and its aptamer and the formation of TdT-derived DNA-template AgNCs, we fabricate a series of CoA-targeted electrochemical biosensors and their electrochemical performances are first investigated by cyclic voltammetry (CV) and electrochemical impedance spectroscopy (EIS). Figure 2A displays the CVs obtained by four different modified electrodes in $[Fe(CN)_6]^{3-/4-}$ solution. It can be observed that the peak current of Electrode 3 is lower than other electrodes, which can be ascribed to the repulsive force between the TdT-extended long DNA and the electrochemical $[Fe(CN)_6]^{3-/4-}$ probe. Moreover, the potential differences of the two peaks become larger and larger along with assembly procedures, implying further the electrochemical sensor is assembled successfully. Meanwhile, EIS, as an effective technique to explore the electron transfer properties and interfacial properties of

surface modified electrode, is used for supporting the fabrication of the biosensor as well. Figure 2B illustrates the EIS plots of four different electrodes and the impedance value increases continuously in the assembly process. Meanwhile, as shown in the inset of Figure 2B, the EISs after and before the AgNCs formation in Electrode 3 preparation process are exhibited, and the impedance value decreases significantly after the formation of DNA-AgNCs, which can be basically ascribed to the fact that AgNCs facilitate the electron-transfer. These results demonstrate that the aptasensor has been accomplished successfully.

To verify whether the proposed aptasensor indeed worked as expected, SWV is used to characterize the changes of the stripping signal after each modification step. As shown in Figure 2C, only weak signals are observed for Au, Electrode 1 and Electrode 2, but the signal for Electrode 3 is very obvious at about +0.15 V, which is the typical stripping peak of silver (Jin et al., 2018). Then, compared with Electrode 3, there are negligible electrochemical signals without TdT extension (Figure S2), the main reason is that Ag(I) possesses a preferred high affinity to cytosine base (C) over adenine (A), guanine (G) and thymine (T) bases (Han et al., 2012; Yuan et al., 2014). Next, we find also a significant electrochemical response in the presence of CoA (Figure 2D). At this point, the aptasensor is successfully fabricated as expected, and it can be employed for investigating CoA analysis favourably.

(Figure 2)

3.3. Detection of HAT p300 and its inhibitors

Given those factors, the sensitivity and dynamic range of the electrochemical aptasensor are explored by detecting a series of CoA standard solutions with SWV technique. As shown in Figure S3A, the increasing response currents are observed with the increment of CoA concentration from 0 to 120 μM. Simultaneously, a linear relationship is obtained between increasing current response and CoA concentrations ranging from 0.1 μM to 100 μM (Figure S3B), and the detection limit is 0.016 μM (according to 3δ/slope, δ is the standard deviation of the blank samples). Additionally, the specificity of our aptasensor is investigated by replacing CoA with other similar molecules including mercaptoacetic (MPA), cysteine (Cys), glutathione (GSH), adenosine triphosphate (ATP), adenine and nucleotide (AMP) under the same analysis condition. As shown in Figure S3C, only CoA reveals a significant current signal, whereas, the current signals of other substances are approximately the same as that of blank. Furthermore, to test the true potential in the following HAT detection, some requisites of HAT reaction are added to discuss the practicability. As depicted in Figure S3D, the stripping current of sole peptide or HAT or Ac-CoA is as same as the blank, but the one of the mixtures is similar to the one of CoA. All above results reveal that our method is reliable for CoA analysis, and could be applied for subsequent CoA-supported HAT analysis. When CoA-Ag(I) coordination polymer (CP) is present, there is a significant electrochemical response and fluorescence enhancement (Figure S4). In view of the unique property of CoA-Ag(I) CP, the two methods above are also used for investigating CoA generated by the acetylation reaction. As we expected, some significant results under the generating CoA after

acetylation are in accord with the ones under pure CoA (Figure S5). These results illustrate the HAT-generated CoA can trigger hopefully the fabrication of the proposed biosensor, achieving the detection of HAT p300.

It is well known that experimental conditions have an effect on the sensitivity of the sensor. To better achieve the detection of HAT p300, we investigate the effects of incubation time (Figure S6A) and incubation temperature (Figure S6B) for the HAT reaction, the concentration of the used Ac-CoA (Figure S6C), pH for the HAT reaction buffer (Figure S6D) and the concentration of the used Ag(I) (Figure S6E). The best optimal values for incubation time, incubation temperature, Ac-CoA concentration, pH of the reaction buffer and Ag(I) concentration are found to be 80 min, 30 °C, 1 mM, pH 7.0 and 100 μM, respectively, and more detailed discussions have been placed in supporting information.

Based on the optimal detection conditions, the CoA-aptamer-facilitated SWV biosensor is firstly employed for sensitive HAT p300 activity detection. Figure 3A shows the peak value at +0.15 V in SWV increases gradually with the increasing p300 concentration from 0 to 500 nM. A linear relationship between the peak current and the logarithm of HAT p300 concentration (lgC_{p300}) is displayed in the range from 0.01 to 100 nM (Figure 3B) with a detection limit of 0.0028 nM determined by 3δ/slope (δ, standard deviation of the blank samples). Table S2 summarizes a comparison of the analytical performances of other HAT-related methods for the detection of p300. As a result, the sensitivity of CoA-aptamer-facilitated SWV biosensor is comparable or

better than that of some previous correlative work, exhibiting an excellent performance.

Selectivity is a key index for evaluating our new CoA-aptamer-facilitated HAT biosensor, especially potential application in subsequent biological samples. The selectivity of the aptasensor to HAT p300 is conducted by using HRP, CHY, UDG, AChE, PKA, and ChOx as control. As shown in Figure 3C, only when HAT p300 exists in the reaction solution, a relatively strong electrochemical signal appears. And other substances lead to negligible current enhancement at the same conditions, suggesting good selectivity in discriminating target and others. Furthermore, compared with HAT p300, negligible changes of the electrochemical signal for a series of mixture are observed (Figure 3D), showing a great potential for HAT sample analysis.

(Figure 3)

Inhibition of HAT p300 activity is in connection with the occurrence and development of major diseases involving cancer, diabetes, Alzheimer's disease and cardiovascular diseases, and so on. Considering that it, the HAT inhibitors including anacardic acid and C646 are evaluated by our strategy. Figure 4A depicts the current response gradually decreases by the increasing anacardic acid concentration, this is to say there is a rising gradually inhibition efficiency (Figure 4B), and the half-maximal inhibitory concentration (IC_{50}) is 13.03 μM, which is analogous to previous reports (Chen et al., 2015; Hu et al., 2015). Moreover, C646 is also investigated in our HAT p300 reaction system (Figure 4C). C646-induced phenomena are consistent with what

we already know referring to anacardic acid and the IC_{50} value is determined to be 1.15 μM (Figure 4D), which corresponds with that reported in the literature (Li et al., 2016; Wang et al., 2017; Warner et al., 2016). The above results clearly demonstrate that our new method can be used to screen qualitatively HAT p300 inhibitors.

(Figure 4)

3.4. Stability, reproducibility, and sample analysis

The long-term storage stability of the CoA-aptamer-facilitated HAT biosensor, as another key factor, is evaluated by measuring some electrodes every week. As illustrated in Figure 5A, their peak currents keep off 99.7%, 97.5%, 93.2% and 85.9% of original ones after one, two, three or four weeks, respectively, indicating that this biosensor might be suitable for long-distance transport and detection. Next, the reproducibility of the aptasensor is also tested under the four concentrations and keep for five times parallel detection (Figure 5B), obtaining some relative standard deviations which are lower than 5%.

Reliability and application potential of a new analytical method should be assessed in the real biological samples. Hence, the proposed biosensor is performed for HAT p300 analysis in Hela cell lysates (Figure 5C) and serum samples (Figure 5D) at different volume ratios, displaying some ignorable differences. It can be seen from Table S3, the lysates and serum samples are also detected with a recovery of 99.8% to 104.4% and a RSD less than 5%. All above results indicates that the new CoA-aptamer-based biosensor can be applied for HAT-related real sample analysis.

(Figure 5)

4. Conclusions

To summarized, a new, simple and label-free electrochemical SWV biosensor has been developed for HAT detection coupled with a CoA and its aptamer system. After HAT reaction, the generated CoA can induce the conformational change of CoA-aptamer, resulting in the formation of C-rich DNA by the extension of TdT. The subsequent C-rich DNA-templated AgNCs serve as the SWV stripping signal output. The proposed biosensor offers a sensitive and selective analysis for HAT detection with a detection limit of 0.0028 nM. Meanwhile, the biosensing strategy can be also applied for HAT-related inhibitors analysis. This work presents a new approach to develop a new kind of aptamer-facilitated biosensor for HAT detection. After advancement in biosensing technology, we believe that our biosensor can be commercialized and applied for anti-carcinogenic drug discovery and clinical diagnosis.

Acknowledgements

Financial support from the National Natural Science Foundation of China (21605089 and 81773483), the Ningbo Municipal Natural Science Foundation (2017A610231 and 2018A610217), the Open Subject of State Key Laboratory of Chemo/Biosensing and Chemometrics (2016001 and 2017016), Zhejiang Provincial Natural Science Foundation of China (LGF18B070002), State Key Laboratory for Quality and Safety of Agro-products (ZS20190101) and State key Laboratory of Analytical Chemistry of Life Science (SKLACLS1804) are gratefully acknowledged.

This work was also sponsored by K.C. Wong Magna Fund in Ningbo University.

References

Ahmadyousefi, Y., Malih, S., Mirzaee, Y., Saidijam, M., 2019, Biochimie 156, 1-11.

Ait-Si-Ali, S., Ramirez, S., Robin, P., Trouche, D., Harel-Bellan, A., 1998, Nucleic Acids Res. 26, 3869-3870.

Akki, S.U., Werth, C.J., 2018, Environ. Sci. Technol. 52, 8989-9007.

Asadian, E., Ghalkhani, M., Shahrokhian, S., 2019, Sensor. Actuat. B-Chem. 293, 183-209.

Barker, G.C., Gardner, A.W., 1992, Analyst 117, 1811-1828.

Bennett, S.A., Tanaz, R., Cobos, S.N., Torrente, M.P., 2019, Transl. Res. 204, 19-30.

Chen, H.J., Liu, X., Li, W., Peng, Y., Nie, Z., 2019, Biosens. Bioelectron. 126, 535-542.

Chen, S.Y., Li, Y., Hu, Y.F., Han, Y.T., Huang, Y., Nie, Z., Yao, S.Z., 2015, Chem. Commun. 51, 4469-4472.

Chuh, K.N., Batt, A.R., Pratt, M.R., 2016, Cell Chem. Biol. 23, 86-107.

Compton, P.D., Kelleher, N.L., Gunawardena, J., 2018, J. Proteome Res. 17, 2727-2734.

Espiritu, C.A.L., Justo, C.A.C., Rubio, M.J., Svobodova, M., Bashammakh, A.S., Alyoubi, A.O., Rivera, W.L., Rollon, A.P., O'Sullivan, C.K., 2018, ACS Infect. Dis. 4, 1306-1315.

Ghadiali, J.E., Lowe, S.B., Stevens, M.M., 2011, Angew. Chem. Int. Ed. 50,

3417-3420.

Goda, E.S., Gab-Allah, M.A., SyduluSingu, B., RoYoon, K., 2019, Microchem. J. 147, 1083-1096.

Han B., Wang E., 2012, Anal. Bioanal. Chem. 402, 129-138.

Han, Y.T., Li, H., Hu, Y.F., Li, P., Wang, H.X., Nie, Z., Yao, S.Z., 2015, Anal. Chem. 87, 9179-9185.

Hu, Y.F., Chen, S.Y., Han, Y.T., Chen, H.J., Wang, Q., Nie, Z., Huang, Y., Yao, S.Z., 2015, Chem. Commun. 51, 17611-17614.

Hu, Y.F., Zhang, Q.Q., Hu, D.D., Wang, J., Rao, J.J., Xu, L.H., Guo, Z.Y.,Wang, S., Liu, X., Tang, S.Y., Shen, Q.P., 2019, Microchim. Acta 186, 325.

Jin, X., Zhou, L., Zhu, B., Jiang, X., Zhu, N., 2018, Biosens. Bioelectron. 107, 237-243.

Langelier, M.F., Eisemann, T., Riccio, A.A., Pascal, J.M., 2018, Curr. Opin Struc. Biol. 53, 187-198.

Lee, M.J., Tsai, Y.J., Lin, M.Y., You, H.L., Kalyanam, N., Ho, C.T., Pan, M.H., 2019, Phytomedicine 57, 377-384.

Luan, Y.P., Li, J., Bernatchez, J.A., Li, R.S., 2019, J. Med. Chem. 62, 3171-3183.

Ma, Y., Geng, F.H., Wang, Y.X., Xu, M.T., Shao, C.Y., Qu, P., Zhang, Y.T., Ye, B.X., 2019, Biosens. Bioelectron. 134, 36-41.

Magiera, M.M., Singh, P., Gadadhar, S., Janke, C., 2018, Cell 173, 1323-1327.

McCullough, C.E., Marmorstein, R., 2016, ACS Chem. Biol. 11, 632-642.

Miao, X.Y., Wang, Y., Gu, Z., Mao, D.S., Ning, L.M., Cao, Y., 2019, Anal. Bioanal.

Chem. 411, 387-393.

Michaelides, M.R., Kluge, A., Patane, M., Van Drie, J.H., Wang, C., Hansen, T.M., Risi, R.M., Mantei, R., Hertel, C., Karukurichi, K., Nesterov, A., McElligott, D., de Vries, P., Langston, J.W., Cole, P.A., Marmorstein, R., Liu, H., Lasko, L., Bromberg, K.D., Lai, A., Kesicki, E.A., 2018, ACS Med. Chem. Lett. 9, 28-33.

Nie, Y.M., Yuan, X.D., Zhang, P., Chai, Y.Q., Yuan, R., 2019, Anal. Chem. 91, 3452-3458.

Qi, H.S., Zheng, W.W., Zhang, C., Zhou, X., Zhang, L., 2019, ACS Appl. Mater. Inter. 11, 12846-12853.

Sen, P., Lan, Y.M., Li, C.Y., Sidoli, S., Donahue, G., Dou, Z.X., Frederick, B., Chen, Q.J., Luense, L.J., Garcia, B.A., Dang, W.W., Johnson, F.B., Adams, P.D., Schultz, D.C., Berger, S.L., 2019, Mol. Cell 73, 684-698.

Singh, N.K., Chakma, B., Jain, P., Goswami, P., 2018, ACS Comb. Sci. 20, 350-357.

Vázquez-González, M., Willner, I., 2018, Langmuir 34, 14692-14710.

Wang, H.X., Li, Y., Zhao, K.L., Chen, S.Y., Wang, Q., Lin, B., Nie, Z., Yao, S.Z., 2017, Biosens. Bioelectron. 91, 400-407.

Weerathunge, P., Ramanathan, R., Torok, V.A., Hodgson, K., Xu, Y., Goodacre, R., Behera, B.K., Bansal, V., 2019, Anal. Chem. 91, 3270-3276.

Xu, L.H., Zhang, Q.Q., Hu, Y.F., Ma, S.H., Hu, D.D., Wang, J., Rao, J.J., Guo, Z.Y., Wang, S., Wu, D., Liu, Q., Peng, J.Q., 2019, Anal. Chim. Acta 1066, 28-35.

Yuan Z., Chen Y., Li H., Chang H., 2014, Chem. Commun. 50, 9800-9815.

Yan, J.H., Xiong, H.J., Cai, S.D., Wen, N.C., He, Q.Y., Liu, Y.F. Peng, D.M., Liu, Z.B.,

2019, Talanta 200, 124-144.

Yin, Z.Z., Wang, S.H., Shen, B.C., Deng, C.Y., Tu, Q.Y., Jin, Y., Shen, L., Jiao, B., Xiang, J., 2019, Anal. Chem. 91, 3539-3545.

Zhang, W., Dixon, M.B., Saint, C., Teng, K.S., Furumai, H., 2018, ACS Sensors 3, 1233-1245.

Zhu, G.Z., Chen, X.Y., 2018, Adv. Drug Deliver. Rev. 134, 65-78

Zou, Y., Wang, Z.H., Zhang, H.X., Liu, Y., 2018, Biosens. Bioelectron. 122, 205-210.

Zou, Y., Zhang, H.X., Wang, Z.H., Liu, Q.Y., Liu, Y., 2019, Talanta 198, 39-44.

Zucconi, B.E., Makofske, J.L., Meyers, D.J., Hwang, Y.S., Wu, M.X., Kuroda, M.I., Cole, P.A., 2019, Biochemistry 58, 2133-2143.

Figure Caption

Scheme1. Schematic illustration of Coenzyme A-aptamer-facilitated label-free electrochemical stripping strategy for sensitive detection of histone acetyltransferase activity.

Fig.1. Fluorescence quenching effect of GO: (A) Interaction of FAM-labeled DNA1, DNA2, DNA3 or CoA-aptamer-1 and CoA molecule; (B) Specificity on CoA by replacing target by other similar substances (100 μM); (C) Concentration influence of 1 and 100 μM CoA; (D) The change of fluorescence signal under different NaCl concentrations (10, 30, 50, and 100 mM).

Fig.2. (A) CVs and (B) EISs for different modified electrodes in 5 mM $[Fe(CN)_6]^{3-/4-}$ containing 0.1 M KCl; SWVs in PBS (100 mM, pH 7.0) for (C) different assembled electrodes and (D) the proposed biosensor in absence or presence of 100 μM CoA.

Fig.3. (A) SWV responses of the aptasensor for different concentrations of p300: 0, 0.01, 0.015, 0.02, 0.05, 0.1, 0.2, 0.5, 1.0, 2.0, 5.0, 10, 20, 50, 100, 200, 500 nM and (B) the corresponding calibration plots; (C) Specificity and (D) anti-interference of the aptasensor against different enzymes, the concentrations of all substances are 100 nM.

Fig.4. (A) SWV responses of the aptasensor for different concentrations of anacardic acid concentrations: 0, 0.1, 0.2, 0.5, 1, 2, 5, 10, 20, 40, 80, 100, 150, 200, 500, 1000 μM and (B) the inhibition assay for HAT p300 as a function of anacardic acid concentrations; (C) SWV responses of the aptasensor for different concentrations of C646 concentrations: 0, 0.01, 0.02, 0.05, 0.1, 0.2, 0.5, 1, 2, 5, 10, 20, 40, 80, 120, 200

μM and (D) the inhibition assay for HAT as a function of C646 concentrations. [HAT p300] = 100 nM.

Fig.5. (A) The stability of the proposed electrochemical aptasensor examined every week; (B) reproducibility of the proposed electrochemical HAT p300 aptasensors; HAT p300 detection in different volume ratios (5%, 10%, or 30%) of (C) Hela cell lysates and (D) serum samples; [HAT p300] = 100 nM.

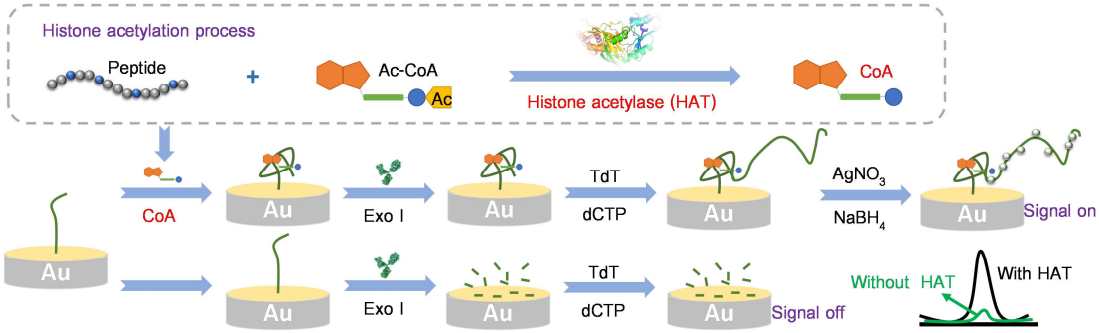

Scheme1. Schematic illustration of Coenzyme A-aptamer-facilitated label-free electrochemical stripping strategy for sensitive detection of histone acetyltransferase activity.

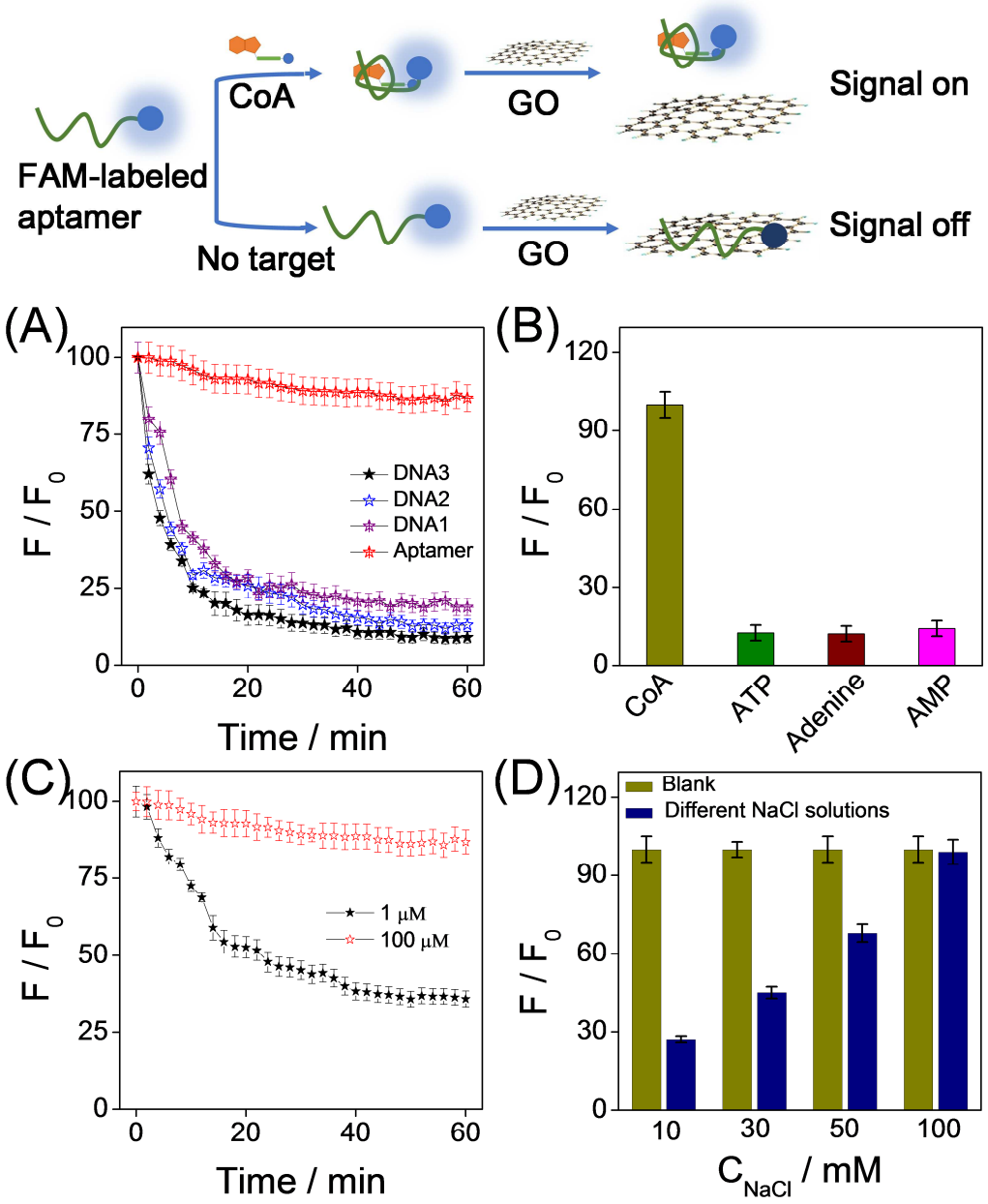

Fig.1. Fluorescence quenching effect of GO: (A) Interaction of FAM-labeled DNA1, DNA2, DNA3 or CoA-aptamer-1 and CoA molecule; (B) Specificity on CoA by replacing target by other similar substances (100 μM); (C) Concentration influence of 1 and 100 μM CoA; (D) The change of fluorescence signal under different NaCl concentrations (10, 30, 50, and 100 mM).

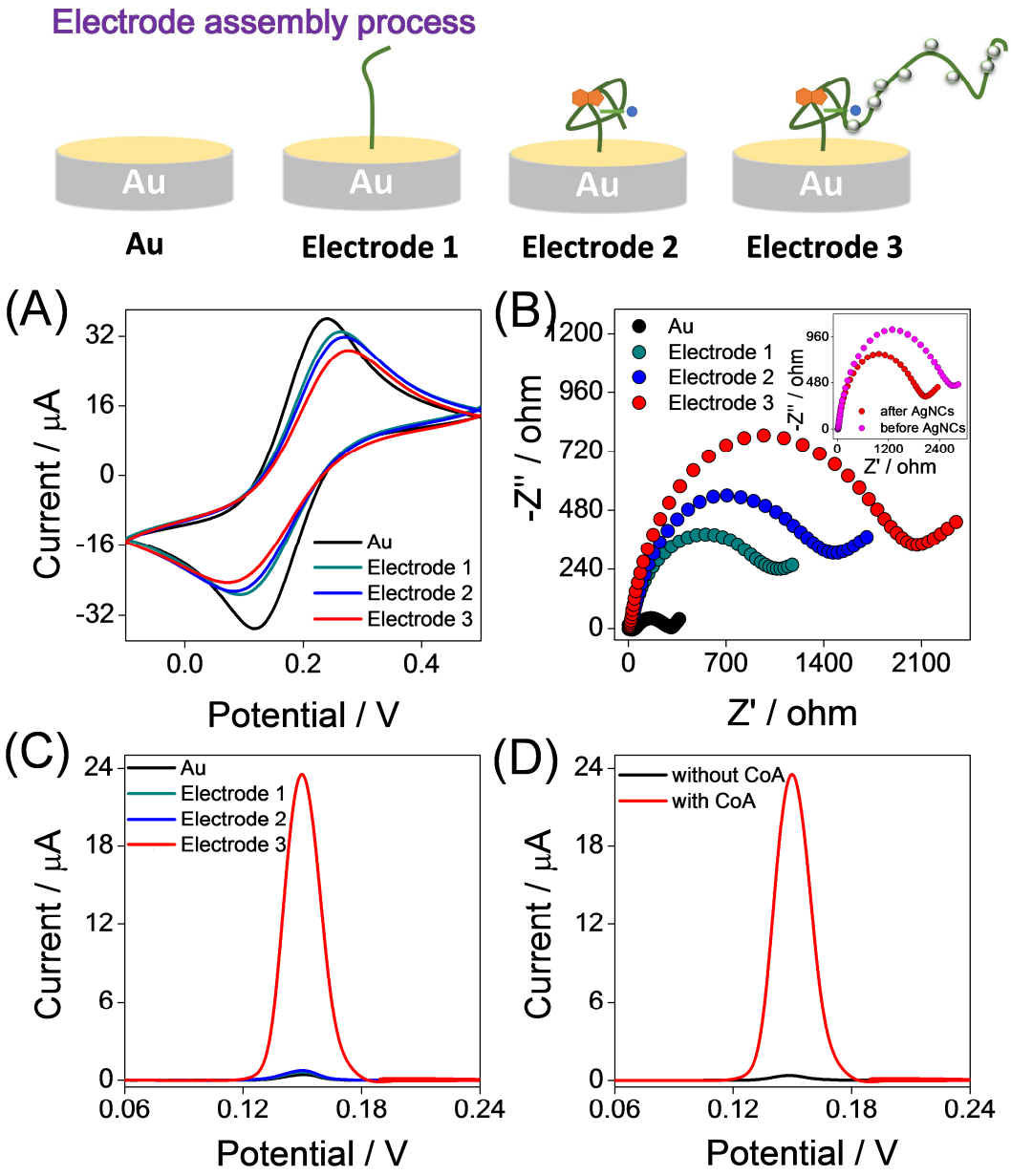

Fig.2. (A) CVs and (B) EISs for different modified electrodes in 5 mM $[Fe(CN)_6]^{3-/4-}$ containing 0.1 M KCl, inset: EISs before and after the AgNCs formation in Electrode 3 preparation process; SWVs in PBS (100 mM, pH 7.0) for (C) different assembled electrodes and (D) the proposed biosensor in absence or presence of 100 μM CoA.

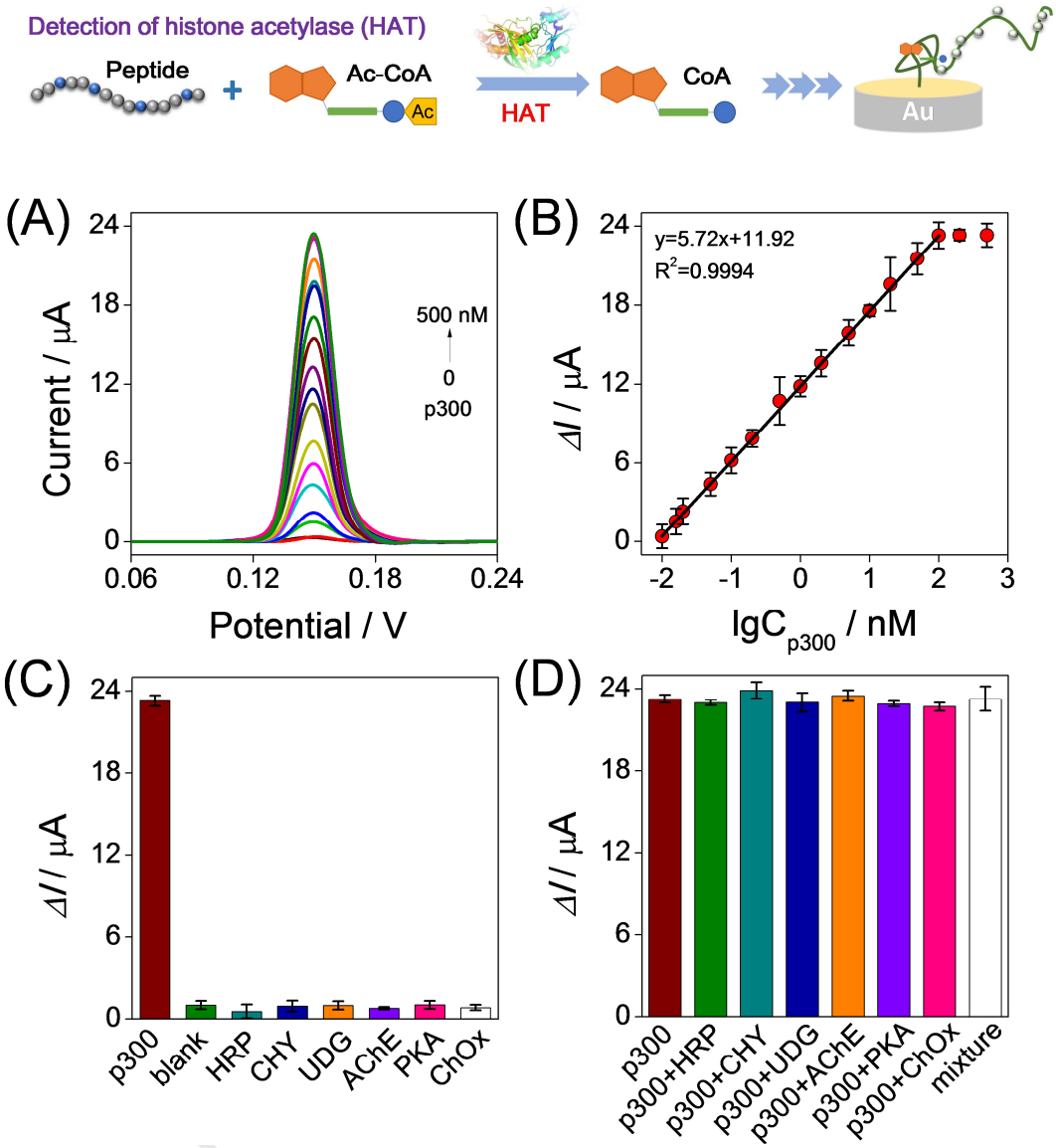

Fig.3. (A) SWV responses of the aptasensor for different concentrations of p300: 0, 0.01, 0.015, 0.02, 0.05, 0.1, 0.2, 0.5, 1.0, 2.0, 5.0, 10, 20, 50, 100, 200, 500 nM and (B) the corresponding calibration plots; (C) Specificity and (D) anti-interference of the aptasensor against different enzymes, the concentrations of all substances are 100 nM.

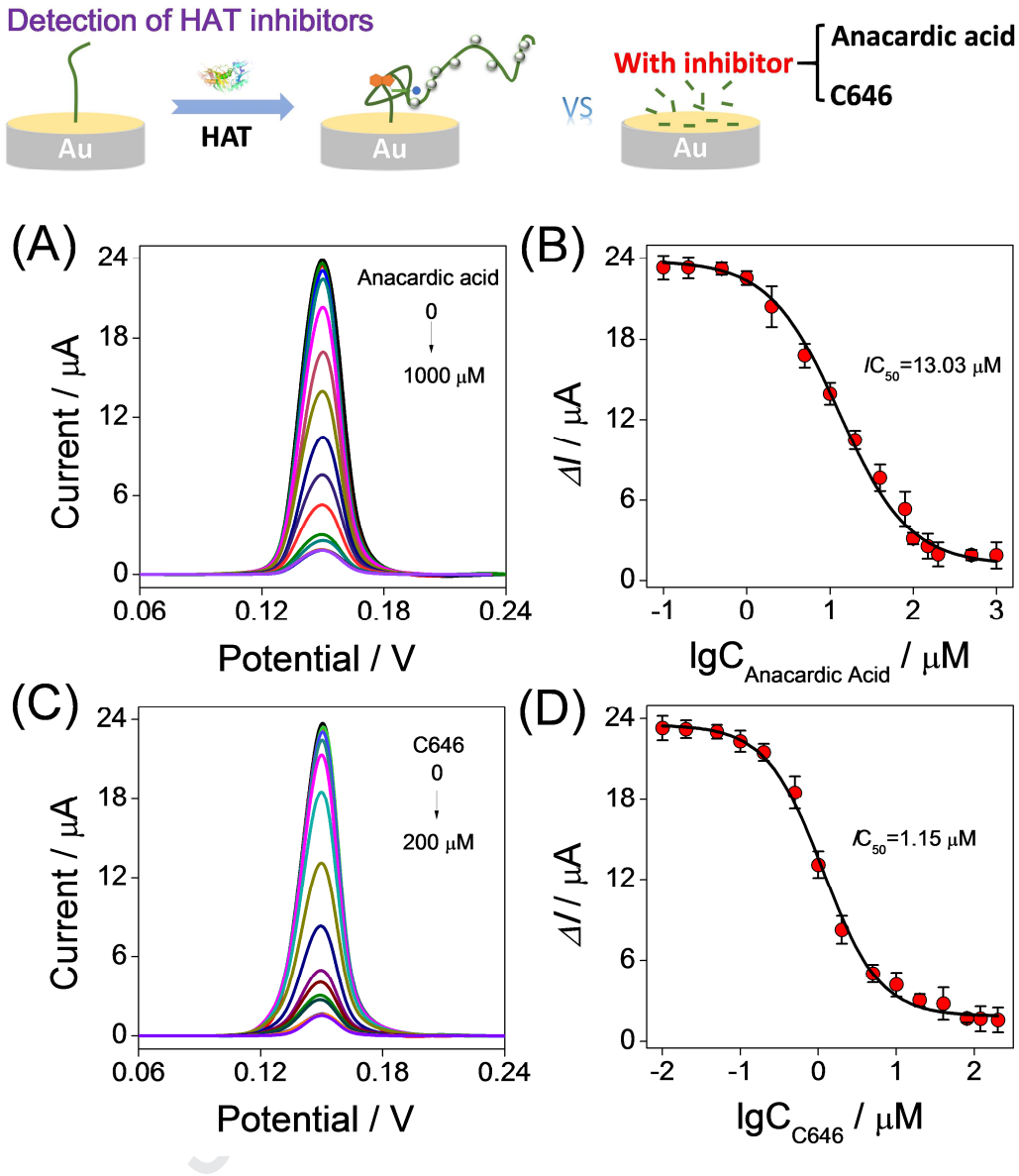

Fig.4. (A) SWV responses of the aptasensor for different concentrations of anacardic acid concentrations: 0, 0.1, 0.2, 0.5, 1, 2, 5, 10, 20, 40, 80, 100, 150, 200, 500, 1000 μM and (B) the inhibition assay for HAT p300 as a function of anacardic acid concentrations; (C) SWV responses of the aptasensor for different concentrations of C646 concentrations: 0, 0.01, 0.02, 0.05, 0.1, 0.2, 0.5, 1, 2, 5, 10, 20, 40, 80, 120, 200 μM and (D) the inhibition assay for HAT as a function of C646 concentrations. [HAT p300] = 100 nM.

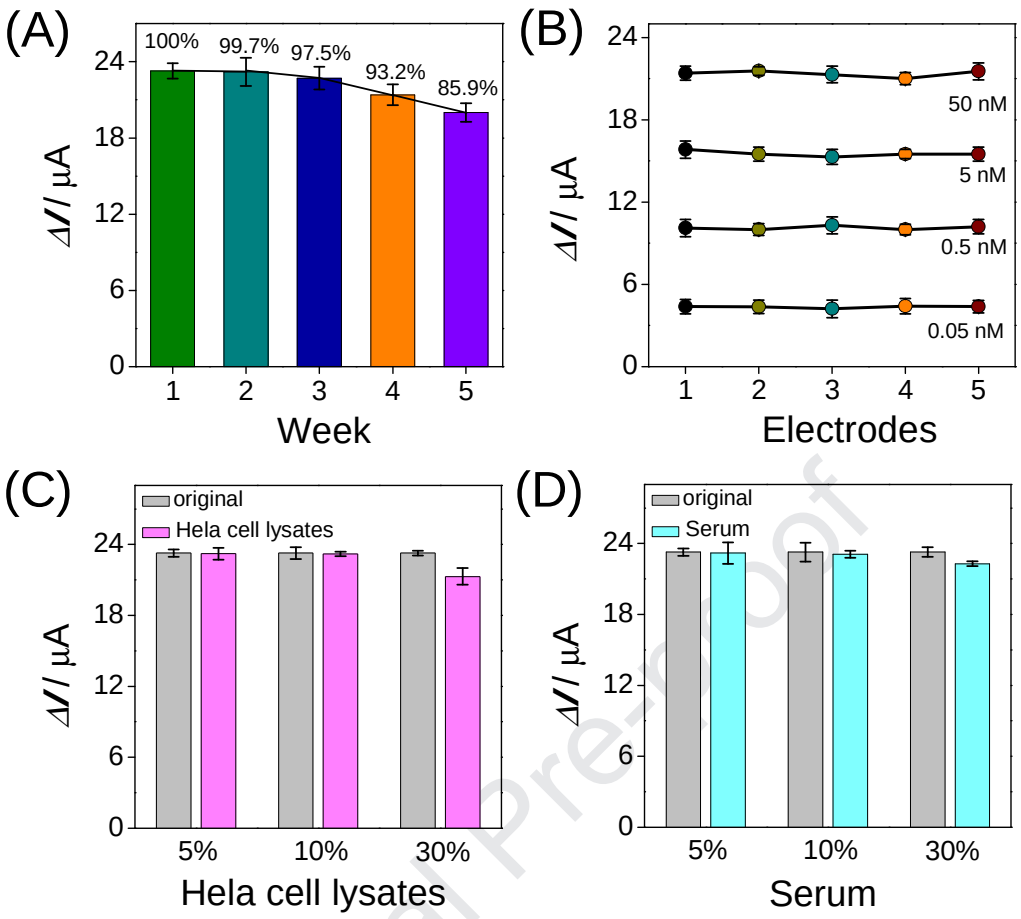

Fig.5. (A) The stability of the proposed electrochemical aptasensor examined every week; (B) reproducibility of the proposed electrochemical HAT p300 aptasensors; HAT p300 detection in different volume ratios (5%, 10%, or 30%) of (C) Hela cell lysates and (D) serum samples; [HAT p300] = 100 nM.

Highlights

- A novel SWV stripping strategy for HAT p300 analysis is first presented.
- Interaction of Coenzyme A and its aptamer first serves as an initiator.
- TdT-induced silver nanoclusters act as electrochemical signal resources.
- The biosensor is exploited for HAT p300 and its inhibitors detection.
- The platform shows great potential applications in real biological sample.

Author contribution

Author	Contribution
Dandan Hu	Preparation and Characterization of the biosensor
Yufang Hu	Design of the biosensing strategy and writing of this paper
Tianyu Zhan	Synthesis of Materials
Yudi Zheng	PAGE, AFM, and TEM Characterization
Pingjian Ran	Activity detection
Xinda Liu	Inhibitors detection
Zhiyong Guo	Fluorescence detection
Wenting Wei	Optimization experiment
Sui Wang	Sample analysis

Author Biographies

Dandan Hu is a postgraduate student in the School of Materials Science and Chemical Engineering, Ningbo University. Her research interests include biosensors and materials.

Yufang Hu received her PhD degree in State Key Laboratory of Chemo/Biosensing and Chemometrics, College of Chemistry and Chemical Engineering, Hunan University, Changsha, 410082, P. R. China. She has been working in the School of Materials Science and Chemical Engineering, Ningbo University since 2015. Her research interests include biomaterials, nanotechnology, analytical chemistry, and electro-chemistry.

Tianyu Zhan is a postgraduate student in the School of Materials Science and Chemical Engineering, Ningbo University. Her research interests include biosensors and materials.

Tianyu Zhan is a postgraduate student in the School of Materials Science and Chemical Engineering, Ningbo University. Her research interests include biosensors.

Yudi Zheng is an undergraduate student in the School of Materials Science and Chemical Engineering, Ningbo University. Her research interests include biosensors and materials.

Pingjian Ran is an undergraduate student in the School of Materials Science and Chemical Engineering, Ningbo University. Her research interests include biosensors and materials.

Xinda Liu is an undergraduate student in the School of Materials Science and Chemical Engineering, Ningbo University. His research interests include biosensors and materials.

Zhiyong Guo received his PhD degree in chemistry from University of Science and Technology of China in 2005. He has been working in the School of Materials Science and Chemical Engineering, Ningbo University since 2005 and was appointed professor in analytical chemistry in 2012. His research interests include biosensors and electro-analytical chemistry.

Wenting Wei received his PhD degree in College of Chemistry and Chemical Engineering, Hunan University, Changsha, 410082, P. R. China. He has been working in the School of Materials Science and Chemical Engineering, Ningbo University since 2015. His research interests include biomaterials, nanotechnology, and organic synthesis.

Sui Wang received his PhD degree in chemistry from Lanzhou University of China in 2005. He has been working in the School of Materials Science and Chemical Engineering, Ningbo University since 2005 and was appointed associate professor in analytical chemistry in 2007. His research interests include biosensors and electro-analytical chemistry.

Declaration of interests

☐ The authors declare that they have no known competing financial interests or personal relationships that could have appeared to influence the work reported in this paper.

☐The authors declare the following financial interests/personal relationships which may be considered as potential competing interests:

The authors report no conflicts of interest. The authors alone are responsible for the content and writing of this article.